Fe$_2$O$_3$-Au Hybrid Nanoparticles for Sensing Applications via SERS Analysis

Emily Searles[1] and Dr. Simona Hunyadi Murph[1,2]

[1]National Security Directorate, Savannah River National Laboratory, Aiken, SC USA

[2]Department of Physics and Astronomy, University of Georgia, Athens, GA, USA

Corresponding author, email address: Simona.Murph@srnl.doe.gov

Phone: 1-803-646-6761, Fax: 1-803-646-6761

Abstract:

Multifunctional iron oxide-gold hybrid nanostructures have been produced via solution chemistries and investigated for analyte detection. Gold nanoparticles of various shapes have been used for probing surface-enhanced Raman scattering (SERS) effects as they display unique optical properties in the visible-near IR region of the spectrum. When coupled with other nanoparticles, namely iron oxide nanoparticles, hybrid structures with increased functionality were produced. By exploiting their magnetic properties, nanogaps or "hot spots" were rationally created and evaluated for SERS enhancement studies. The "hot spots" were created by using a seeded reaction to increase the gold loading on the iron oxide support by 43% by weight. SERS Nanomaterials were evaluated for their ability to promote surface-enhanced Raman scattering of a model analyte, 4-mercaptophenol. The data shows an enhancement effect of the model analyte on gold decorated iron oxide nanoparticles.

I.   Introduction:

Incident light scatters as it transmits through a chemical species. The extent to which the electric field is distorted, the degree to which the light is scattered, is a measure of the polarizability of the species of interest. (1) By analyzing the extent to which the species scatters light a unique fingerprint of the species can be observed. This fingerprint is derived from the distinctive inelastic collision scattering signal, Raman scattering. Through employing the fingerprint capabilities of Raman scattering an advantageous spectroscopy technique can be derived to provide data on the identity of the analyte. The main obstacle facing this form of analysis is the intensity of the Raman scattering signal. (2). Due to the low intensity scattering signal of the not forbidden but rare occurrence of inelastic collisions during the introduction of incident light, a technique needs to be established to enhance the spectra.

Surface Enhanced Raman Spectroscopy (SERS) is a surface-sensitive analytical technique that enhances Raman scattering of chemical species adsorbed on rough surfaces or nanoscale structures (1). This technique used to observe vibrational, rotational, and other low-frequency modes in a system. It provides s a structural fingerprint by which molecules can be identified. There are two mechanisms to describe the overall SERS enhancement: the electromagnetic (EM) and chemical (CHEM) enhancement mechanisms. EM enhancement is due to the increased local electric field incident on an adsorbed molecule at a metallic surface, due to visible light absorption by the metal. CHEM enhancement results from electronic resonance/charge transfer between a molecule and a metal surface, which leads to an increase in the polarizability of the molecule (18).

The Raman enhancement technique was first observed by Fleischmann's group when on the surface of a silver electrode (2). This enhancement was due to the interaction of the rough metal surface leading to the increase of the inelastic collision signal (2). The presence of the metal surface roughness increased the scattering effect and led to better sensitivity (2). SERS has been a growing chemical field, since the recent advances in the nanoscience and nanotechnology fields, leading to extraordinary results to increase the Raman signal. Enhancements of 10^6 are often claimed, and higher values are seen in specific instances (3). Even single molecule detection was reported by several groups when employing nanoscale materials (3).

Nanoparticles with large amounts of surface area and unique characteristics that are distinct from their bulk material provide an interesting support in the enhancement of inelastic scattering signal. (3) SERS has been explored through using nanoparticles to increase the Raman signal for sensing, bioanalysis, catalytic analysis, and environmental applications (2,3).

Among many properties displayed by gold nanoparticles, one of the most notable is their ability to absorb and scatter light in the visible region of the electromagnetic spectrum. In metal nanoparticles, "plasma oscillations",
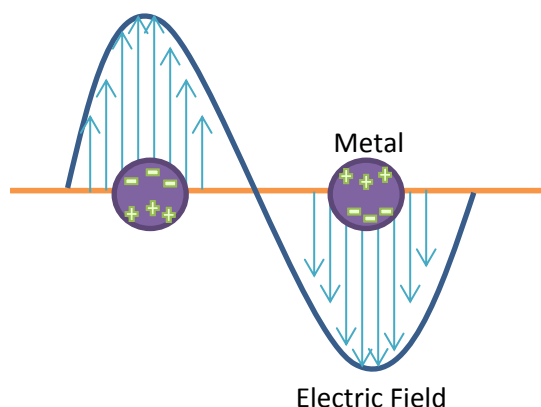

Figure 1: Nanoparticle Localized Surface Plasmon Resonance

which are collective oscillation of electrons, driven by external electromagnetic fields are localized and lead to strong resonances at specific wavelengths that are dependent on the particle size, shape and the local dielectric environment (18). Localized surface plasmon resonance (LSPR) has the greatest contribution to SERS as electrons oscillate around nanoparticle surfaces (3). Large enhancement factors and even single-molecule SERS are expected for molecules at junctions between aggregated nanoparticles [18]. This is a result of localized surface plasmon (LSP) coupling between nanoparticles and enhanced electromagnetic field intensity localized at nanoparticle junctions activated by absorption of visible light (18). These hot spots can be tailored to lead maximum effects by changing the size, shape or location of the (4). Additional improvements can be found by using laser frequencies which are resonant with electronic and vibrational transitions of the analyte, thereby increasing the efficiency of the Raman process. Lasers can therefore match the plasmon band of the nanoparticles increasing the interaction of the plasmon band with the incident light, because lasers can be fabricated in the same wavelength of light as these particles. The LSPR of the nanoparticle can contribute additionally to SERS through ground state interactions, resonant process, photon-driven electron-transfer, and transient electron enriched states (3, 5).

Gold and silver nanoparticles have been widely used for applications in SERS because they demonstrate the greatest effect of plasmonic behavior when compared to other nanoparticles. They are highly stable and their plasmonic properties occur in the visible-near IR range allowing the optical properties to be easily monitored (18, 6). In previous research it has been found bimetallic silver-gold nanowire provides the greatest enhancement when compared to silver nanowires and gold nanotubes (7). This enhancement was attributed to the unique shape of the nanoparticle which allowed a higher tunability to match the wavelength of incident light (7).
        One of the problem associated with the design of such nano-architectures is the ability to produce the particles in a uniform, reproducible way for large scale application.

One way of creating scalable "hot-spot" bearing nanostructures is by using wet chemistry techniques. In this project, we produced "hot-spot" bearing Au-Fe_2O_3 nanostructures by (a) a seed-mediated approach, where Fe_2O_3 served as the seed support, and (b) electrostatic interactions between gold nanorods and iron oxide spheres. Samples were characterized by SEM, EDS, and UV-Vis spectroscopy techniques to elucidate their properties and morphologies. Raman response of a model analyte, 4-mercaptophenol, was evaluated on these structures.

II. Experimental

A. Materials

Chloroauric acid trihydrate, trisodium citrate, iron (III) oxide nanospheres, 4-mercaptophenol, purchased from Sigma Aldrich. All samples were used as received.

B. Nanomaterials Synthesis

1. Seed-Mediated approach of Iron Oxide-Gold Spheres Multifunctional Nanoparticle

Iron oxide-gold hybrid nanostructures were synthesized using a citrate reduction technique as shown in Figure 2. An aqueous stock solution of 20mM Fe_2O_3 nanospheres was prepared using deionized water. The reaction proceed by heating 10 mL of deionized water to a boil, followed by the immediately injection of 1mL of 20mM Fe_2O_3. The solution was allowed to heat for several minutes followed by the addition of 1mL of 1% sodium citrate. Finally, 250 µL of 0.01 M chloroauric acid was added. The solution was heated at 248 °C for approximately 4 minutes as the solution processed through a color change from burnt orange to purple with removal from heat once a red solution was generated. A red colored solution indicates the formation of gold nanospheres. The solution was allowed to cool and was cleaned using a magnet to separate the excess unreactive species and the gold particles not attached on the Fe2O3 support (17).
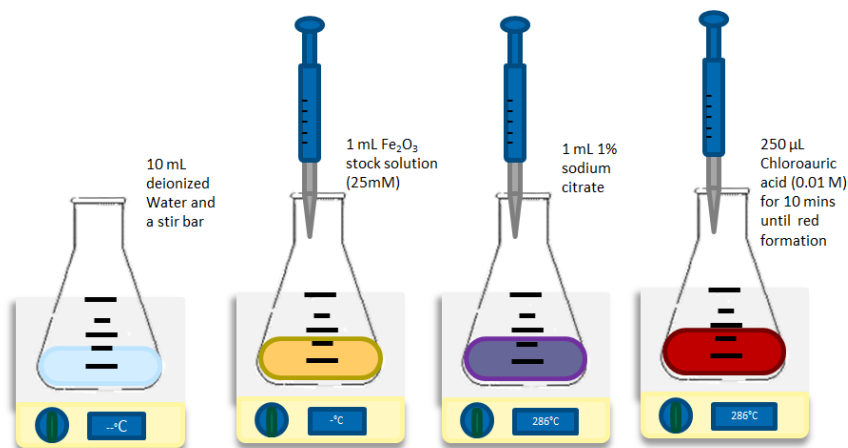

Figure 2: Synthesis of Iron oxide-Gold hybrid nanostructures through citrate reduction

Once separated, these Au-Fe2O3 nanostructures were used as "seeds" in the next step. An identical seed-mediated approach was employed. Five different seedings steps were performed to achieve optimal loading Au nanoparticles loadings on the Fe2O3.

2. Iron Oxide-Gold Rods Multifunctional Nanoparticle Synthesis

Gold rods were attached to iron oxide through electrostatic interactions. Gold rods synthesized with cetyltrimethylammonium bromide (CTAB) using the method previously used in the Murph's lab were used. Iron oxide was treated with chloroauric acid to ensure the particles preserved a negative surface charge. The 0.5mM iron oxide nanospheres, 0.05 M chloroauric acid and concentrated gold nanorods were incubated at room temperature for one hour. These particles were washed and separated with a magnet and analyzed through SEM imaging to ensure electrostatic interactions proved favorable.

C. Attachment of 4-mercaptophenol

A 50mM stock solution of 4-mercaptophenol was prepared in distilled water. Differing amounts: 2, 5, 10, 32 µL, of iron-oxide gold hybrid structures and gold spheres were added to 4-mercaptophenol allowing the solutions to incubate while stirring for 30 minutes before analyzed on Raman spectrometer.

D. Characterization

The gold nanoparticles and iron-oxide gold particles were characterized using a scanning electron microscope (Hitachi SU8320). Energy-dispersive spectroscopy (EDS) was used to determine the material's composition and collect mapping of EDS on the particles using an Oxford XMax 150 mm2 Crystal EDS. To determine surface charge and effective nanoparticle diameters Brookhaven NanoBrook ZetaPALS was used. A Varian, Cary 500 scan UV-Vis-NIR Spectrophotometer was used to monitor nanoparticles' optical properties

E. SERS Analysis

The Raman spectroscopy experiments were run with a Del Mar Photonics, DMPC-532-1 with a beam diameter focused to ~20 µm at a λ=532 nm. A quartz cuvette was used with the laser set on 120mW with collection times of 120 seconds averaged over 5 scans.

III.   Results and Discussions

The scattering of light as a result of the transmittance of an applied electric field through the electron cloud occurs via inelastic and elastic collisions. Rayleigh scattering represents the elastic collision of light where the scattered photon has the same energy as the incident photon. Elastic collisions are the most abundant form of light scattering from the introduction of incident photons. They represent changes in direction of photons not changes in vibrational energy (1).

The energy is conserved in the collision as illustrated in Figure 3. The dipole changes during elastic collisions, however the species has no change in polarizability. Inelastic collisions experience a change in polarizability, producing a unique fingerprint scattering signal that can be matched to a specific element of interest. Raman scattering can be used for analysis of composition and trace analysis of species within complex matrices using the vibrational information (2). However, the Raman signal is weak when compared to Rayleigh scattering. Raman scattering is less likely to occur and when it does it occurs in both Stokes and anti-Stokes forms as illustrated in Figure 3. Stokes scattering occurs when the scattered photon of light is of a lower energy than the incident light. Anti-stokes scattering is observed when the incident
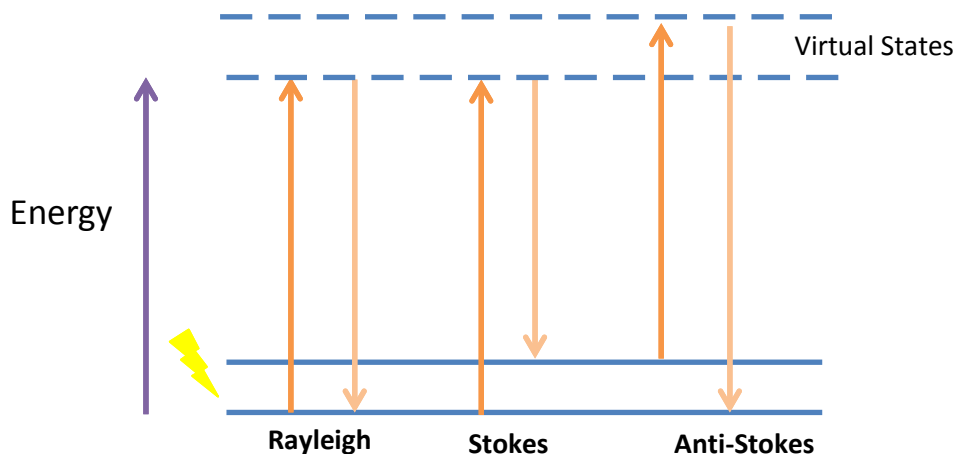
Figure 3: Virtual State Energy Diagram representing Rayleigh elastic collisions and Raman inelastic Stokes and Anti-Stokes collisions

photon of light gains energy. The loss and gain of energy is a result of the excitation of the electron to virtual states, non-quantized short lived energy states, without the conservation of energy from the incident photon.

A. Seed-mediated approach: Iron Oxide Nanoparticles Decorated with Gold

Iron (III) oxide nanospheres with an average diameter of 50 nm were used as a support for gold decoration. Decoration of iron oxide with gold was modeled by the procedure published by Murph et al (17). The formation of this composite structure allows the magnetic properties of the iron oxide along with the plasmonic properties of the gold to be exhibited simultaneously. Once the particles were synthesized they were further characterized by SEM and EDS to elucidate the morphology, loading and composition of the composite structure.

Figure 4 shows a SEM image of the nanoparticles observed. Gold nanospherical particles of 20 nm in diameter were easily grown on the Fe2O3 supports. While not all the gold nanoparticles were deposited on the support, a high
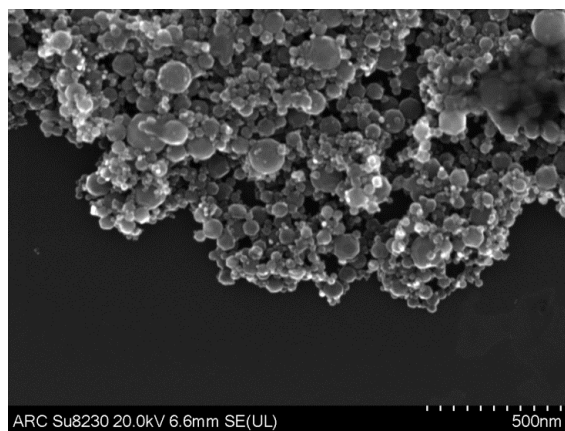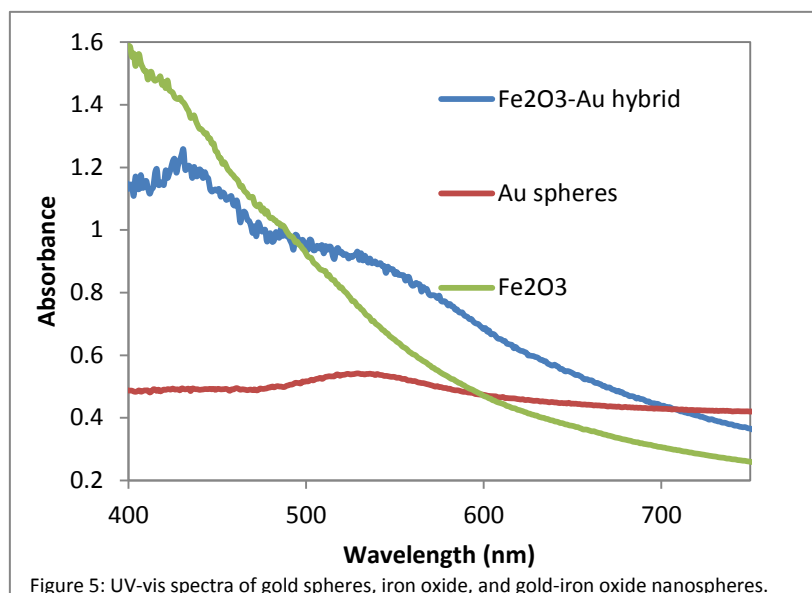
Figure 4: SEM image of gold-iron oxide nanospheres, bright spots correspond to gold while darker areas are iron oxide

Figure 5: UV-vis spectra of gold spheres, iron oxide, and gold-iron oxide nanospheres.

distribution of Au was observed on the majority of the support. Unbound Au nanoparticles were removed from the original solution before characterization.

EDS analysis demonstrated that 12.6 ± 1.9 weight-percent gold were present on the Fe_2O_3. UV-vis spectra, as shown in Figure 5, shows that the iron oxide and gold particles are composite structures; as the iron oxide shows a peak at

420 nm and the gold plasmon band at 520 nm highlighting.. Figure 4 shows the presence of gold on the iron oxide. The first seed mediated approach used shows that the distance between gold nanospheres was too large to provide significant plasmonic interactions, "hot spots", to increase the breathing modes of the SERS analyte for greater enhancement of signal.

To remedy this, increased gold loading was explored through the use of a nanoparticle seeded growth method. This method employed the use of the gold decorated iron oxide particles illustrated in Figure 4 as the support for increased gold loading. In order to create tunable "hot-spots" and nanogaps between gold nanoparticles for sensing application these Au-Fe2O3 nanostructures were further used as seeds to control gold loading on the iron oxide.

The seeded method was applied four times by using the same base Au-iron oxide and adding more gold (III) ions into solution. The first reaction using the seeds increased the weight-
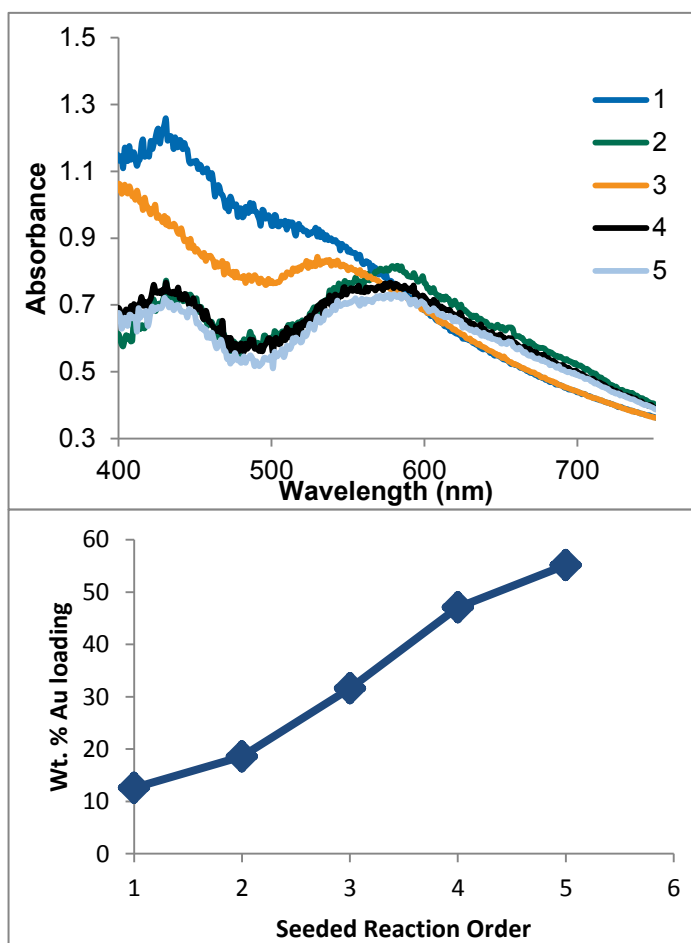

Figure 6: (A) UV-vis spectra of gold-iron oxide nanospheres seeded reaction from original to 4xs seeded. (B) Weight percent loading of increased seeded reactions.

percent loading of gold from 12.6 ± 1.9 mV to 18.6±3.3mV. These results showed that gold loading could be increased through seeded reactions. Further seeded reactions up to four times were found to increase gold decoration of the iron oxide without impacting the integrity of the iron oxide support. UV-vis absorbance of each trial during the seeded reaction shows a more defined gold peak at 520 nm showing a greater decoration on iron oxide as shown in Figure 6A. This increased loading was confirmed by analyzing the weight percent of gold by using EDS. Figure 6B illustrates the tunability of gold loading, namely "hot-spot" creation, through seeded reactions. Figure 7 illustrates comprehensive characterization of the seeded reaction method illustrating the gold loading through EDS mapping, and SEM imaging.
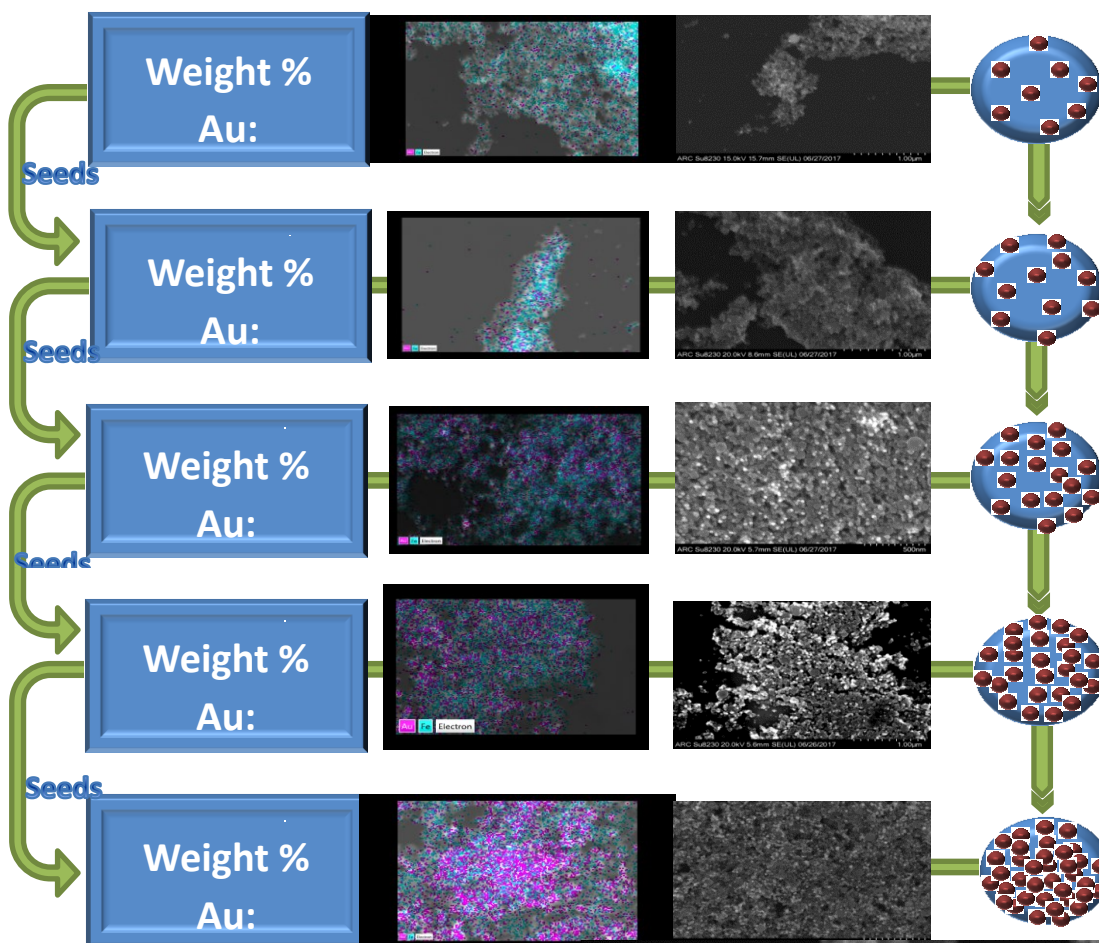

Figure 7: Comprehensive illustration of increased gold load[...] loading capacity, EDS mapping and SEM images.

The final iron oxide-gold hybrid particles with an average of 55.13 weight-percent loading of gold provide a greater opportunity for hot spot and nanogap generation with increased plasmonic characteristics. Figure 8 provides a higher magnification of the iron
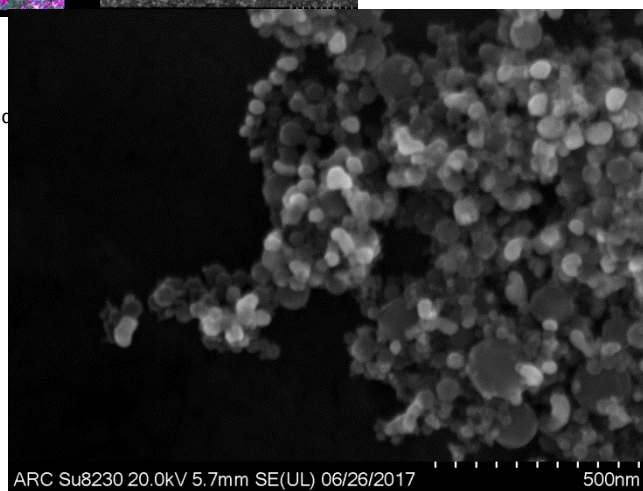

Figure 8: Four times reseeded iron oxide-gold composite structure with increased gold loading.

oxide- gold composite structure to illustrate the remaining integrity of the nanoparticles. Figure 9 further confirms the gold loading of the final seeded particles showing the presence of gold and mapping of the multifunctional structure.

Once iron-oxide gold decorated nanoparticles were found to be reproducibly synthesized further multifunctional composite structures were explored as possible Raman enhancement.
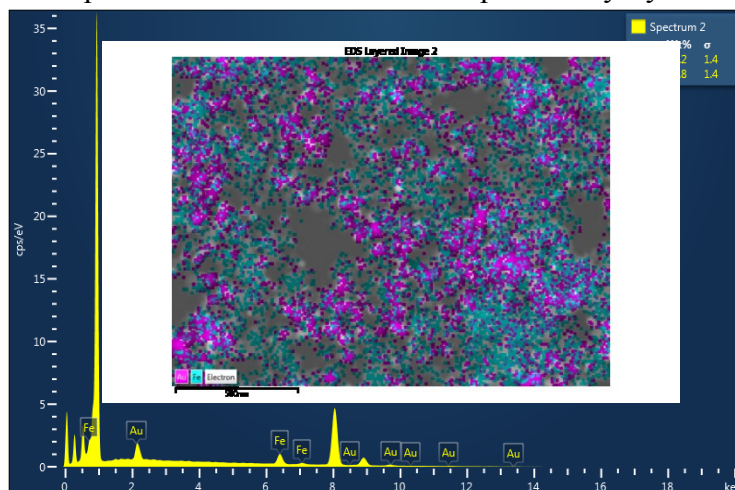

Figure 9: Four times reseeded iron oxide-gold composite structure with increased gold loading EDS mapping and weight percent analysis.

B. Electrostatic Interactions of Gold Rods and Iron Oxide

Gold nanorods, ~18nm in diameter and ~100 nm in length, have also been investigated due to a the "hot-spot" functionality provided at the tips of the particles (7). Spheres exhibit one plasmonic band at 520nm, while rods have two distinct bands due to the transverse and longitudinal plasmon bands at 520 nm and 810nm, as shown in Figure 10. By coupling these "hot-spots" bearing nanorods with the magnetic properties of the iron oxide distinctive applications for SERS analysis may be generated.

The citrate reduction method was not used in the formation of these hybrid structures rather, electrostatic interactions between the already synthesized gold rods and iron oxide spheres were explored to determine a method to provide gold loading suitable for SERS analysis.

The zeta potential of the iron oxide and gold rods was detected

Figure 10: UV-vis absorbance of Gold rods and Gold spheres

separately to determine if the surface charge would provide conditions probable for favorable

electrostatic interactions. The surface charge of the iron oxide nanospheres independently was +42.93± 3.35 mV while the gold rods have a +30mV due to the positively charged cetyltrimethylammonium bromide (CTAB) used in nanorod synthesis. Direct incubation was found to be unfavorable because the surface charges of the individual components were not opposite. Manipulation of the surface charge of the iron oxide was explored to ensure that the particles were negatively charged.

Sodium citrate was first added to iron oxide to attempt to make the surface charge more negative so the positively charged gold rods would electrostatically interact more favorably. Citrate and iron oxide were allowed to incubate before introducing the gold rods in solution. Once the rods were added the solution was allowed to further incubate and then characterized on the SEM. Figure 11 shows the aggregation of gold rods with little to no attachment to the iron
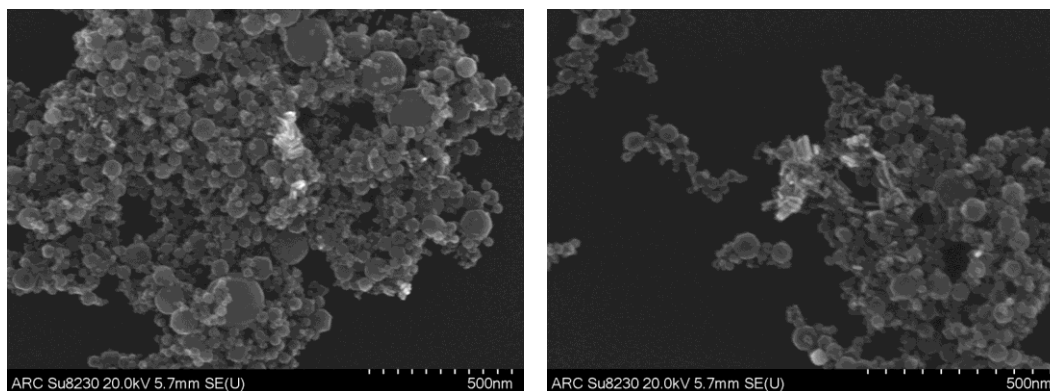

Figure 11: SEM image of sodium citrate incubation of iron oxide with gold rods

oxide support. To try and yield more favorable conditions for gold rod attachment the sodium citrate and iron oxide were heated for promotion of citrate ligand formation. Once the iron oxide and sodium citrate were heated and allowed time for incubation the gold rods were added and allowed to incubate. These SEM images as shown in Figure 12 produced similar results with gold rods aggregation and non-uniform attachment.

Figure 12: SEM image of sodium citrate heated with iron oxide and gold rods
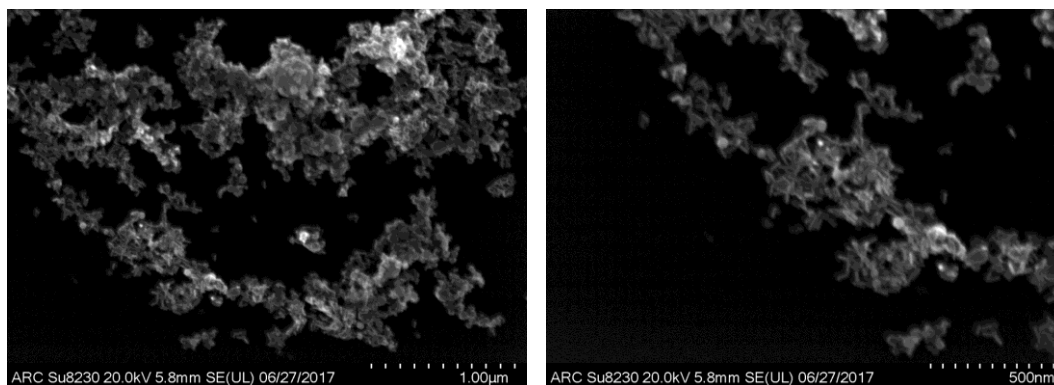
Sodium citrate was determined to not yield favorable conditions for electrostatic interactions between gold rods and iron oxide. The next step to gain promising conditions for gold rod attachment involved the use of chloroauric acid as a salt agent to decrease the surface charge of

the iron oxide. Gold ions were added to iron oxide and at first as shown in Figure 13 the attachment did not prove promising. The attachment was not uniform, however, a higher loading was achieved when compared with sodium citrate incubation approach.
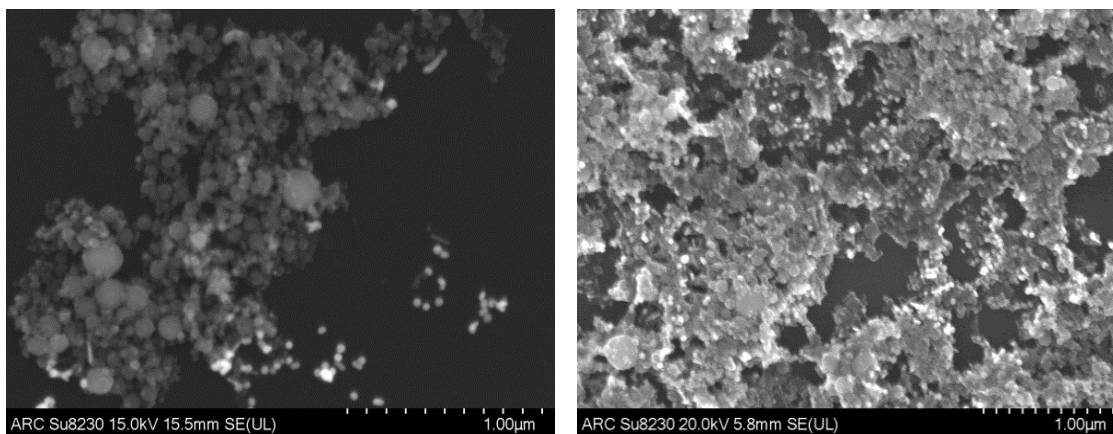

Figure 13: SEM image of gold ions with iron oxide and gold rods

After further work the amount of gold ions added to iron oxide was increased and loading was found to be more favorable with better attachment as shown in Figure 14.
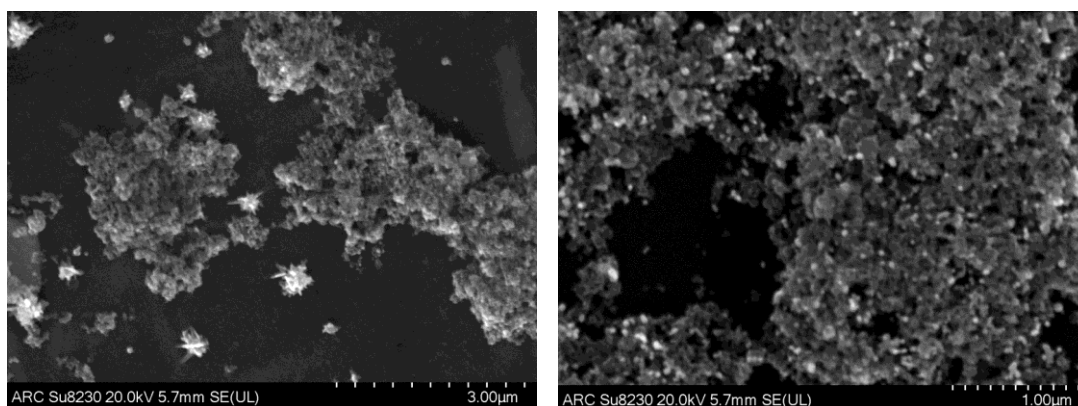

Figure 14: SEM image of gold ions at a higher concentration with iron oxide and gold rods

Interestingly, the gold ions did form micro sized spiky morphologies in solution when not cleaned with a magnet. This suggests that gold ions are being reduced in the presence of the other nanostructures. Upon further analysis of the gold ions in solution galvanic reduction reactions were found to be taking place on the SEM copper grids when the gold ions were not removed from solution through the use of the magnetic cleaning method. The galvanic reduction formed nanocubes on the surface of the copper grids showing the reductive nature of the gold nanoparticles as illustrated in Figure 15.
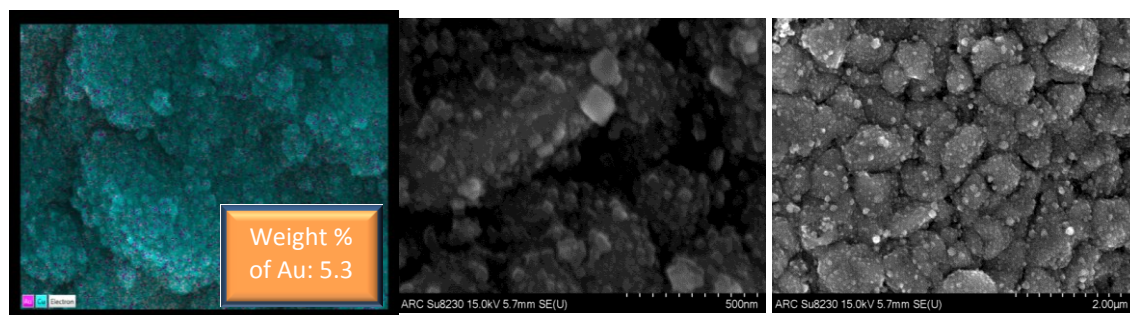
Figure 15: EDS mapping of gold on copper grid surface and weight percent loading of gold ,
SEM image of gold ions causing galvanic reduction reaction on surface of copper grid

The ability to clean the particles by using a magnet removed the excess gold ions that were no longer needed in the tuning of the zeta potential of the iron oxide. Gold rods and iron oxide were successfully attached through using gold ions to manipulate the surface charge of the iron oxide.

C. Raman Spectroscopy

Once the hybrid nanoparticles were synthesized the structures were tested for SERS abilities using a Raman spectrometer data analyzer coupled to a laser. The samples prepared for analysis are shown in Figure 16. The 4-mercaptophenol binds through the sulfide group to the gold nanoparticle on the hybrid composite structures (7). The ring-breathing modes of the 4-mercaptophenol display changes in the polarizability and can be observed in Raman scattering signals at approximately 1100, 1175 and 1260cm^{-1} (7,16). By using 4-mercaptophenol Raman enhancement can be monitored while maintaining a controlled environment of the analyte of interest.
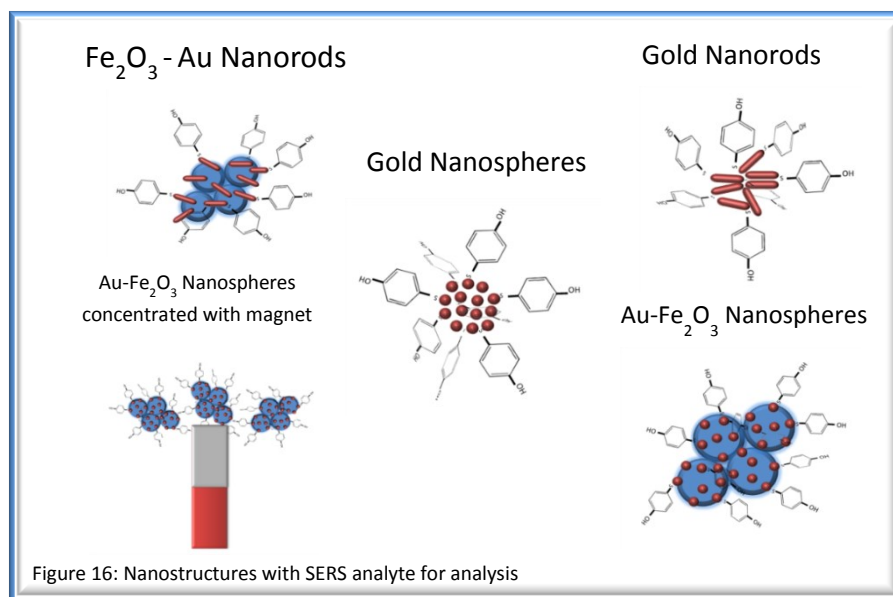

Figure 16: Nanostructures with SERS analyte for analysis

The SERS analyte, 4-mercaptophenol was added to the nanoparticle solutions and allowed time for incubation. To ensure that the thiol bond from the sulfide group to the nanoparticle was formed the surface charge of the nanoparticles were taken before and after the addition of 4-mercaptophenol. Table 1 outlines the change in zeta potential with both the addition of the SERS analyte to gold spheres and iron oxide-gold multifunctional structures with each becoming more positive as 4-mercaptophenol was added.

.

Table 1: **Surface Charge (mV)**	
Fe_2O_3-Au	-24.38±-1.90
Fe_2O_3-Au with 4-mercaptophenol	-8.50±0.66
Au spheres	-18.62±-1.46
Au spheres with 4-mercaptophenol	-4.43±-0.35

With positive results of 4-mercaptophenol attachment stock solution of 4-mercaptophenol was analyzed on the Raman spectrometer to determine the peaks of interest for the determination of enhancement once the nanoparticles were added. Figure 17 shows the 4-mercaptophenol signal and identifies the key peak of interest used throughout the Raman study.

Figure 17: 4-mercaptophenol stock solution highlighting analyte peak at 1100 cm^{-1}
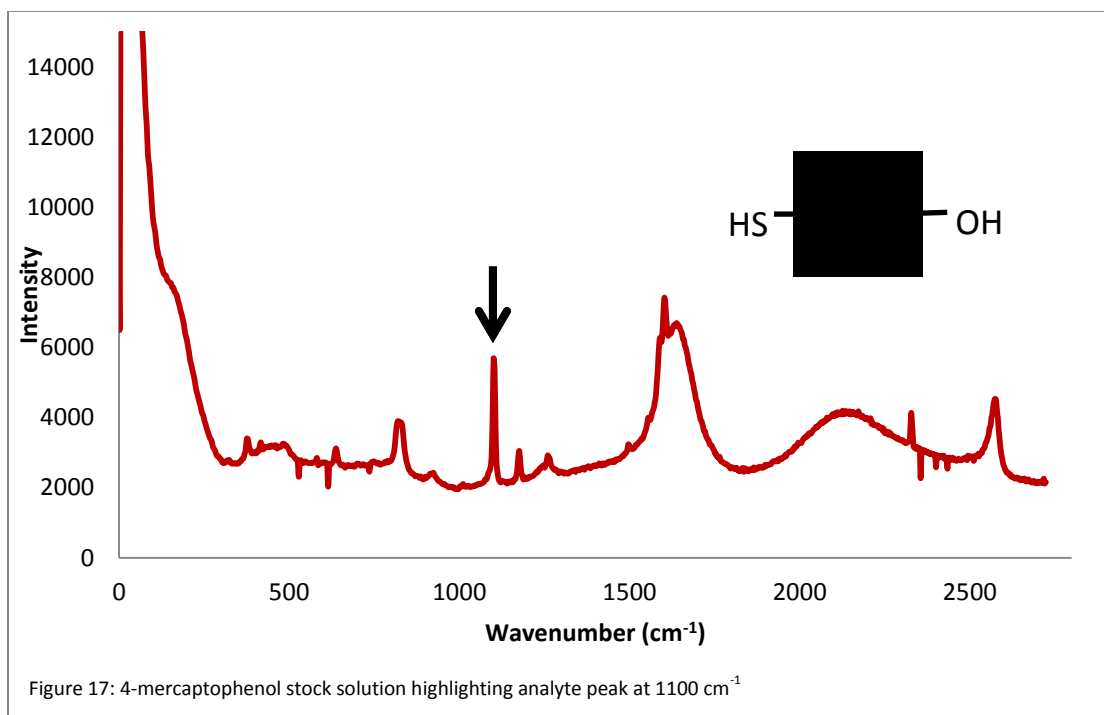
The first Raman test was taken to determine the concentration of 4-mercaptophenol to use throughout the remaining trials. Figure 18 illustrates varying concentrations of the SERS analyte with 10 mM and 5mM 4-mercaptophenol having peaks of the greatest intensity.

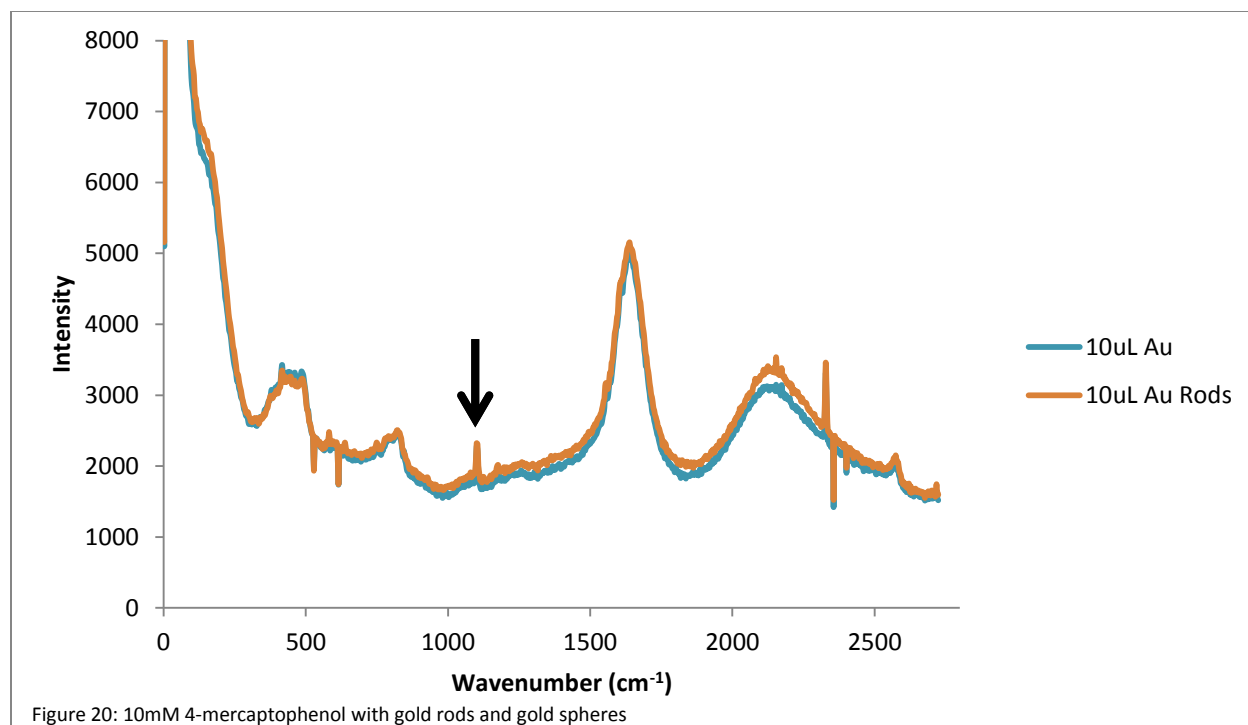Figure 18: 4-mercaptophenol varying concentrations
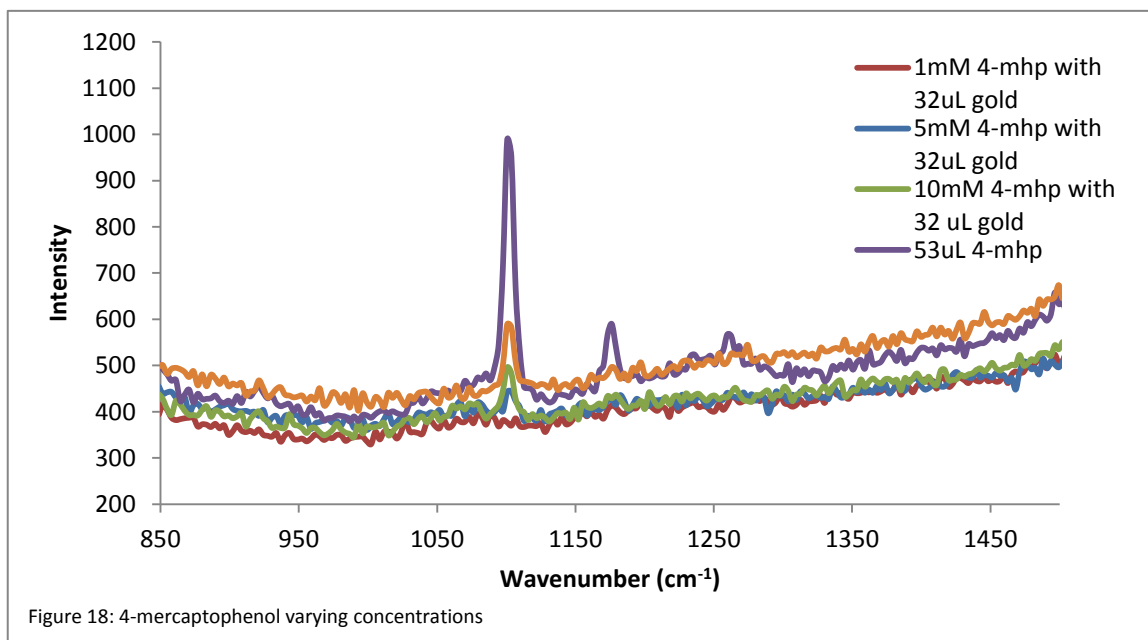
These concentrations were then used throughout the remaining spectroscopic test while varying the amount of gold added to each sample to determine which concentration of gold provided a monolayer of 4-mercaptophenol with direct enhancement from plasmonic properties from gold.

The amount of gold added to the final 1 mL sample was altered to determine the best ratio of gold to 4-mercaptophenol. As shown in Figure 19 multiple amounts of the 1.5×10^{-6} mM gold spheres was added to 10mM 4-mercaptophenol.

Figure 19: 10mM 4-mercaptophenol with varying concentrations of gold spheres
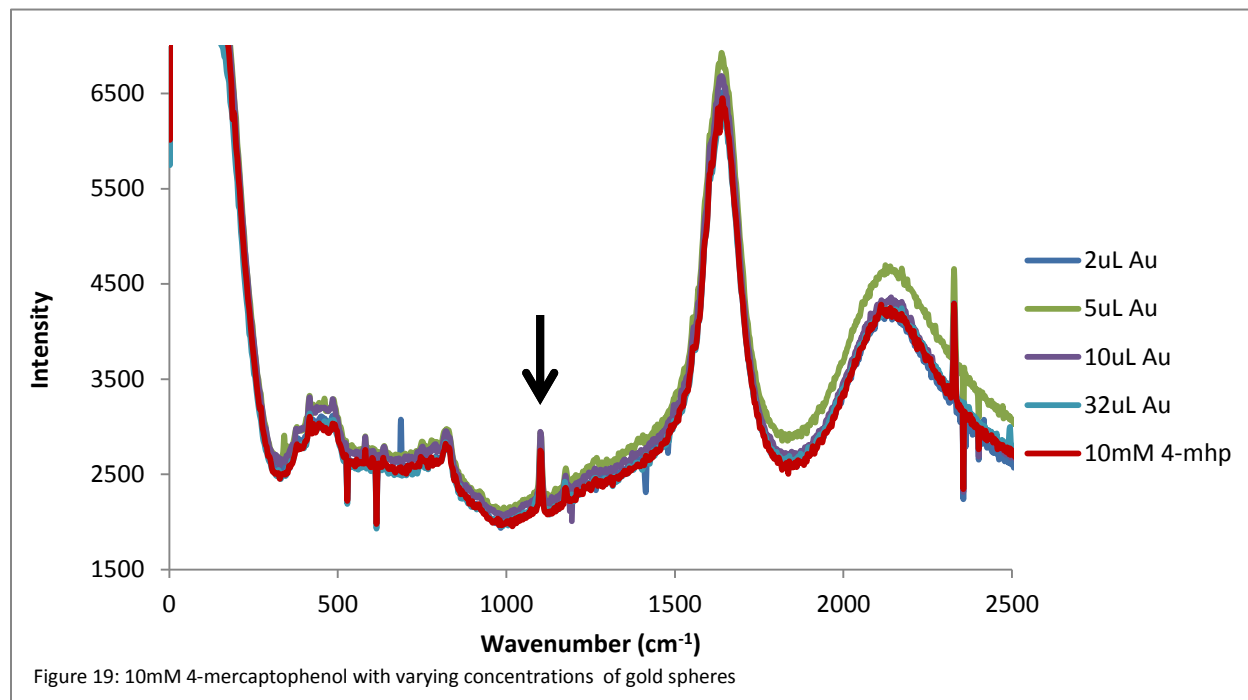
The sample with 10μL gold spheres showed a slight enhancement from the 10mM of 4-mercaptophenol with no gold, showing promising results that enhancement may be found at particular conditions. Figure 20 compares the gold spheres to the gold rods showing a slight increase in signal with the gold rods but not to the extent that would be expected with an additional plasmon band present. This may be attributed to the concentration of gold rods being smaller than that of gold spheres, further studies are needed to determine if the gold rods at higher concentrations would increase the Raman signal of the breathing modes of the 4-mercaptophenol.

Figure 20: 10mM 4-mercaptophenol with gold rods and gold spheres

Similar trials were performed with 5mM 4-mercaptophenol and varying concentrations of iron oxide-gold. Figure 21 illustrates the complete trial while Figure 22 shows the enhancement in signal provided with 10 µL gold spheres and iron oxide gold composite structures.

Figure 21: 5mM 4-mercaptophenol with iron oxide-gold multifunctional nanostructures
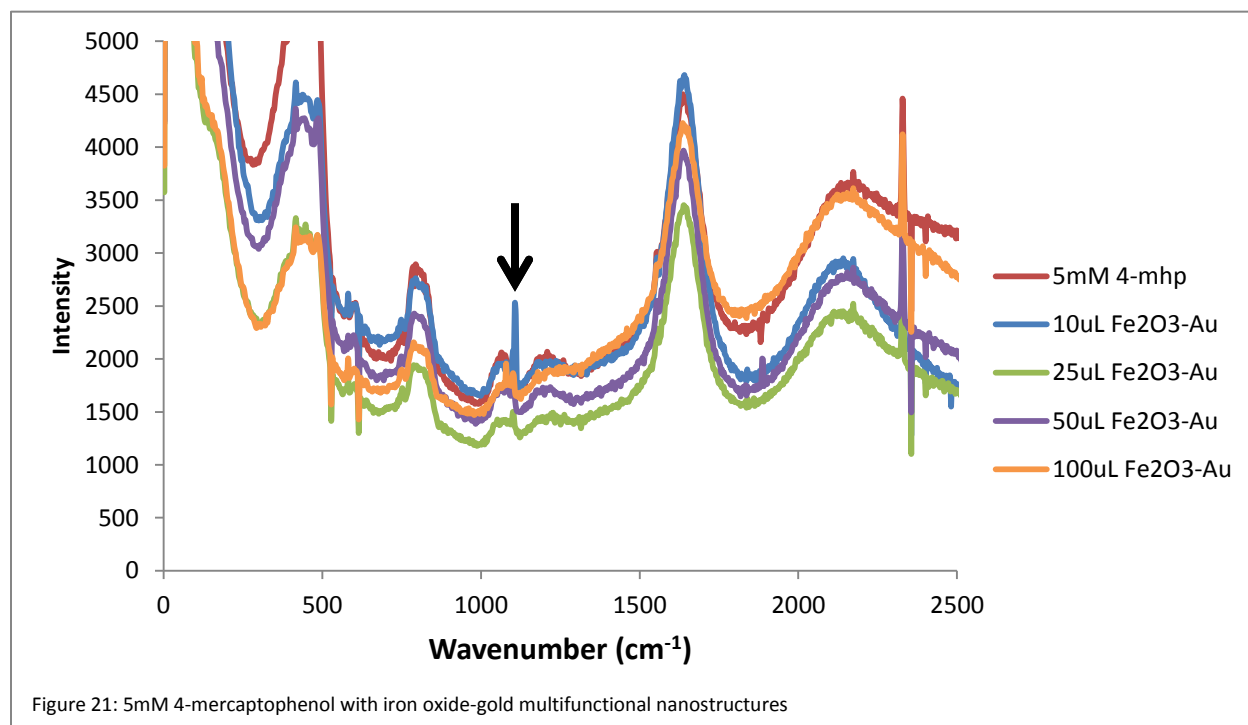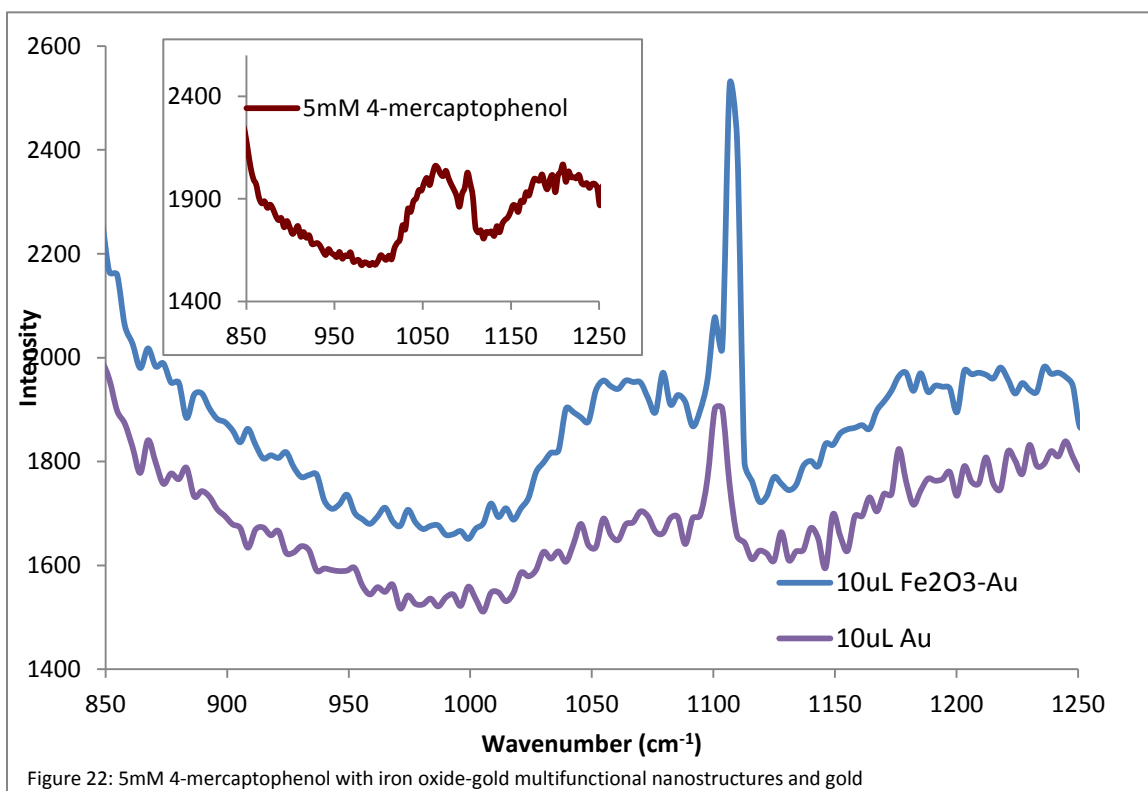
Figure 22: 5mM 4-mercaptophenol with iron oxide-gold multifunctional nanostructures and gold

Raman spectroscopy provided preliminary results of small levels of enhancement from the presence of gold plasmonic particles both on iron oxide supports and independently in solution. The greater increase in signal found in the presence of iron oxide may be attributed to the formation of hot spots on the surface of the iron oxide creating nanogaps at the junctions between gold nanospheres. This technique of the formation of hot spots on the magnetic surface of iron oxide needs further investigation to draw conclusive results of the significance of nanogaps and to determine the tunability of the nanogap through magnetic manipulation.

D. Conclusions

Multifunctional particles with plasmonic and magnetic properties from gold and iron oxide respectively, were reproducibly synthesized through a seeded reaction. Iron oxide-Au loading was significantly increased through the use of seeds during the citrate reduction reaction with a 43% increase in gold loading from the original seeds to those seeded four times. Gold rods were successfully attached to iron oxide through electrostatic interactions with manipulation of surface charge through the addition of Au (III) ions. These particles are not only promising in applications in SERS analysis but may prove to have further applications because of the loading capacity of gold on iron oxide. Composite structures with plasmonic and magnetic properties provide unique characteristics from bulk material including the ability for magnetic manipulation to allow the recyclability of the nanoparticle structure for use in future reactions, reducing cost and use of precious metals such as gold. Raman Spectroscopy identifies SERS analyte and shows slight enhancement, however for larger enhancement desired for SERS more trials must be executed to procure the ideal parameters for large scale application. Future work includes further analysis of the ideal concentrations of SERS analyte coupled with nanoparticles as well

as method development for a more reproducible method for magnetic concentration of iron oxide-gold particles for Raman analysis. Overall, this work successfully synthesized and characterized composite nanostructures that proved to have unique particles from bulk. Applications of these particles for SERS analyte detection require further work to conclusively suggest that such particles reproducibly provide signal enhancement for fingerprint recognition of trace elements in solution.

E. Acknowledgments

F. References

1. Mayo, D.W.; Miller, F.A.; Hannah, R.W. Course Notes on the Interpretation of Infrared and Raman Spectra. Wiley-Interscience. John Wiley and Sons Inc. **2003.**

2. Kawata, S.; Ichimura, T.; Taguchi, A.; Kumamoto, Y. Nano-Raman Scattering Microscopy: Resolution and Enhancement. *Chem. Rev.* **2017,** 117, 4983-5001. http://pubs.acs.org/doi/abs/10.1021/acs.chemrev.6b00560

3. Li, J.F.; Zhang, Y.J.; Ding, S.Y.; Panneerselvam, R.; Tian, Z.Q. Core-Shell Nanoparticle-Enhanced Raman Spectroscopy. *Chem.Rev.* **2017,** 117, 5002-5062. http://pubs.acs.org/doi/ipdf/10.1021/acs.chemrev.6b00596

4. Chen, H.Y.; Lin, M.H.; Wang, C.Y.; Chang, Y.M.; Gwo, S. Large-Scale Hot Spot Engineering for Quantitative SERS at the Single-Molecule Scale. *J. Am. Chem. Soc.* **2015,** 137, 13698-13705.

5. Willets, K.A.; Van Duyne, R. Localized Surface Plasmon Resonance Spectroscopy and Sensing. *Annu. Rev. Phys. Chem.* **2007,** 58, 267-297. http://sites.northwestern.edu/vanduyne/files/2012/10/2007_Willets.pdf

6. Riveria, V.A.G.; Ferri, F.A.; Marega Jr., E.; Localized Surface Plasmon Resonances: Noble Metal Nanoparticle Interaction with Rare-Earth Ions. Intech, Chapter 11. **2012.**

7. Hunyadi, S.E.; Murphy, C.J. Bimetallic silver-gold nanowires: fabrication and use in surface-enhanced Raman scattering. *J. Mater.Chem.* **2006,** 16, 3929-3935.

8. Nam, J.M.; Oh, J.W.; Lee, H.; Suh, Y.D. Plasmonic Nanogap-Enhanced Raman Scattering with Nanoparticles. *Acc. Chem. Res.* **2016,** 49, 2746-2755. http://pubs.acs.org/doi/pdf/10.1021/acs.accounts.6b00409

9. Tian, Y., Chen, L., Zhang, J.; Ma, Z.; Song, C. Bifunctional Au-nanorod@Fe_3O_4 Nanocomposites: Synthesis, Characterization, and their use as Bioprobes. *Nanopart Res*. **2012**, 14, 998.

10. Gao, Q.; Zhao, A.; Guo, Xucheng.; Gan, Z.; Tao, W.; Zhang, M.; Wu, R.; Li,Z. Controlled synthesis of Au-Fe_3O_4 hybrid hollow spheres with excellent SERS activity and catalytic properties. *Dalton Trans.* **2014,** 43, 7998-8006.http://pubs.rsc.org/-/content/articlehtml/2014/dt/c4dt00312h

11. Larsen, G.K.; Farr, W.; Hunyadi Murph, S. Multifunctional Fe_2O_3-Au Nanoparticles with Different Shapes: Enhanced Catalysis, Photothermal Effects, and Magnetic Recyclability. *J. Phys. Chem.* **2016,** 120, 15162-15172.

12. Jain, T.; Tang, Q.; Bjornholm, T.; Norgaard, K. Wet Chemical Synthesis of Soluble Gold Nanogaps. *Acc. Chem. Res.* **2014,** 47, 2-11.

13. Zhang, L.; Xu, J.;Mi, L.; Gong, H.; Jiang, S.; Yu, Q. Multifunctional magnetic-plasmonic nanoparticles for fast concentration and sensitive detection of bacteria using SERS. *Biosens. Bioelectron.* **2012,** 31, 130-136. http://www.sciencedirect.com/science/article/pii/S0956566311006737

14. Li, J.; Skeete, Z.; Shan, S.; Yan, S.; Kurzatkowska, K,; Zhao, W.; Ngo, Q.M.; Holubovska, P.; Luo, J.; Hepel, M.; Zhong, C.J. Surface Enhanced Raman Scattering Detection of Cancer Biomarkers with Bifunctional Nanocomposite Probes. *Anal. Chem.* **2015,** 87, 10698-10702.

15. Barriet, D.; Yam, C.M.; Shmakova, O. E.; Jamison, A.C.; Lee, T. R. 4-mercaptophenylboronic acid SAMs on Gold: Comparison with SAMs Derived from Thiophenol, 4-Mercaptrophenol, and 4-Mercaptobenzoic Acid. *Langmuir.* **2007,** 23, 8866-8875.

16. Orendorff, C.J.; Gole, A.; Sau, T.K.; Murphy, C.J. Surface-Enhanced Raman Spectroscopy of Self-Assembled Monolayers: Sandwich Architecture and Nanoparticle shape dependence. *Anal. Chem.* **2005, 77,** 3261-3266.

17. Hunyadi Murph, S.E.; Larsen, G. K.; Lascola, R.J. Multifunctional Hybrid Fe_2O_3-Au Nanoparticles for Efficient Plasmonic Heating. *J.Vis.Exp.* **2016,** 108.

18. Simona E. Hunyadi Murph, George K. Larsen, Kaitlin J. Coopersmith, Anisotropic and Shape-Selective Nanomaterials: Structure-Property Relationships, 1st ed. 2017, Springer International Publishing, ISBN: 978-3-319-59661-7 (Print) 978-3-319-59662-4 (Online)